The Effects of Heterogeneities and Wavy Interfaces on Capillary Barrier Performance

Clifford K. Ho and Stephen W. Webb
Sandia National Laboratories
Albuquerque, New Mexico 87185
ckho@sandia.gov, swwebb@sandia.gov

Abstract

The performance of capillary barriers with heterogeneities and wavy interfaces has been investigated by numerically simulating three systems comprised of a fine soil layer overlying a coarse gravel layer with 1) homogeneous, 2) layered heterogeneous, and 3) random heterogeneous property fields. The amount of lateral diversion above the coarse layer under steady-state infiltration conditions was compared among the simulations. Results indicated that the performance of capillary barriers can be significantly influenced by the spatial variability of hydraulic properties. Simulations of capillary barriers have also been performed using non-uniform interfaces between the fine and coarse layers. "Wavy" interfaces have been generated using periodic functions of varying amplitude and frequency. Preliminary results of these simulations indicated that breakthrough into the coarse layer was contained primarily in the troughs of wavy interfaces, which may prove useful in waste isolation by providing drainage points between waste packages.

1. Introduction

Engineered and natural capillary barriers in the subsurface have been suggested as an effective means of diverting water away from buried waste. These capillary barriers generally consist of two or more interspersed sloping layers of fine and coarse porous materials (such as sand or soil). Under unsaturated conditions, the capillary pressures in the fine layer are large relative to the capillary pressures in the coarse layer. Therefore, water can be held in fine layers overlying coarse layers. If the layers are tilted, water can be diverted down-dip along the interface of the two layers. This phenomenon has applications and significant impacts in fields including nuclear waste management [*Prindle and Hopkins*, 1990; *Ross*, 1990; *Wilson*, 1996], landfill cover design [*Morris and Stormont*, 1997; *Webb et al.*, 1997], and soil remediation [*Ho and Udell*, 1992].

To date, nearly all of the predictive models that have been used to assess the performance of capillary barriers have assumed that the regions comprising the fine and coarse layers are homogeneous [*Ross*, 1990; *Prindle and Hopkins*, 1990; *Oldenburg and Pruess*, 1993; *Wilson*, 1996; *Webb*, 1996; *Webb*, 1997; *Selker*, 1997; *Warrick et al.*, 1997]. The assumption of homogeneous materials allows uniform, smooth interfaces between the fine and coarse layers, which may over-predict the diversion capacity of actual heterogeneous systems. Homogeneous models also neglect small scale behavior caused by heterogeneities within each layer that may positively or negatively impact the performance of capillary barriers. Therefore, the purpose of this study is to investigate the impact of various intra-unit heterogeneities and inter-unit interface conditions on the performance of capillary barriers. Three cases are presented that include homogeneous, layered heterogeneous, and random heterogeneous realizations of a system comprised of a fine soil layer overlying a coarse gravel layer. A homogeneous simulation with a wavy interface is also presented.

2. Numerical Approach

The computational domain is two-dimensional and consists of a fine layer of soil (1 m high x 6 m wide) overlying a coarse layer of gravel (0.3 m high x 6 m wide). The domain is discretized into 9750 equally spaced elements that are each 0.02 m high x 0.04 m wide. Boundary conditions include infiltration within each element along the top row at a steady rate of 4.62×10^{-7} kg/sec (1 mm/day), no-flow lateral boundaries, and a saturated boundary that is connected to the ten right-most elements in the bottom row to allow outflow of water. The entire domain is tilted 5 degrees clockwise by rotating the gravity vector in the simulations. Only steady-state conditions are considered.

The numerical code TOUGH2 [*Pruess*, 1991] is used to simulate water movement in the unsaturated domains. In the current studies, the gas phase is passive with a constant temperature and pressure (20°C, 1 bar). Only the transport of liquid water is investigated using the TOUGH2 equation of state module *EOS* 9. Full upstream weighting of the unsaturated conductivity is used in this study.

The properties of the domain are taken from two sources: an internal Sandia National Laboratories (SNL)

Table 1. Parameters used in the simulation of homogeneous and heterogeneous property fields. E is the expected value in real space and μ and σ are the mean and standard deviation in natural log space.

	(Fine Layer)			(Coarse Layer)		
	$E^{\dagger}$	μ	σ	$E^{\dagger}$	μ	σ
porosity	0.4	—	—	0.42	—	—
K_{sat} (cm/sec)	1.43×10^{-4}	-9.10	0.700	10	2.30	6.99×10^{-2}
α (1/cm)	0.021	-4.24	0.864	4.9	1.59	4.52×10^{-3}
β	1.87	0.609	0.184	2.19	0.772	0.157
S_r	0.21	-1.63	0.198	0.012	-5.67	1.58

$^{\dagger}E = \exp(\mu + \sigma^2/2)$

report of typical soils and gravel in Albuquerque, NM [*McTigue, D.F., Moisture Retention Properties of Soils from the Chemical Waste Landfill, Sandia National Laboratories, Albuquerque, NM, internal Sandia Letter Report dated* 12/9/94], and a paper describing capillary barrier experiments performed at SNL [*Stormont*, 1995]. The means, μ, and standard deviations, σ, of four properties (in natural log space) are listed in Table 1 along with the expected mean value, E, in real space. The four properties that are allowed to vary spatially in the simulations include the saturated conductivity, K_{sat} (cm/sec), the van Genuchten curve-fitting parameters for capillary pressure and relative permeability, α and β, and the residual liquid saturation, S_r.

For the homogeneous simulation, the expected values, E, are used for the fine and coarse layers. For the heterogeneous simulations, unconditioned sequential Gaussian simulations are performed using GSLIB [*Deutsch and Journel*, 1992] with subsequent standardization to obtain a standard normal distribution of values for all the elements in the domain. Exponential semivariogram models are used with different ranges and anisotropy factors to produce two distinct fields: 1) a layered heterogeneous field and 2) a random heterogeneous field. Ten realizations of each of the two heterogeneous systems are simulated. The layered heterogeneous fields display horizontal features with an effective range of 3 m and an anisotropy ratio of 100:1 in the x-direction, while the random heterogeneous field contains a "salt and pepper" distribution with an effective range of 0.09 m and an anisotropy ratio of 1:1.

Once the standardized variables have been generated, the means and standard deviations in Table 1 are then used to map the standardized variables, Z, to corresponding properties, X, for the fine and coarse layers of the computational domain using the following transformation:

$$X = \sigma Z + \mu \quad (1)$$

If a standardized variable lies between y = 0 m and y = 0.3 m, the means and standard deviations of the coarse layer are used in Equation 1. If a standardized variable lies between y = 0.3 m and y = 1.3 m, the means and standard deviations of the fine layer are used in Equation 1. Because the mean, μ, and standard deviation, σ, are in natural log space, the real space property values are found by taking the exponent of the property values, X, given in equation (1).

A wavy interface between the fine and coarse layers can be generated with a periodic function, $y_{int}(x)$, that defines the interface y-coordinate as a function of any x-coordinate:

$$y_{\text{int}}(x) = A\cos\left(\frac{2n\pi x}{L}\right) + y_1 \quad (2)$$

where A is the amplitude of the "wave", n is the frequency, L is the total width of the domain (6 m), and y_1 is the y-coordinate of the origin of the interface (0.3 m). If the y-coordinate of an element is less than $y_{int}(x)$, then properties of the coarse layer are assigned. If the y-coordinate of an element is greater than $y_{int}(x)$, then properties of the fine layer are assigned. An example of the wavy interface model is applied to the homogeneous model and is presented at the end of the next section.

3. Numerical Results and Discussion

Steady-state liquid saturations and mass flows are simulated for all realizations of the heterogeneous and homogeneous property fields. Saturations and mass flow vectors are plotted for one realization of each of the layered heterogeneous and random heterogeneous fields in Figure 1 along with homogeneous results to illustrate general features. Recall that the infiltration along the top row of elements is constant and that the domain is tilted 5 degrees clockwise. Also, it is worth noting that the criterion for steady-state conditions is that the mass

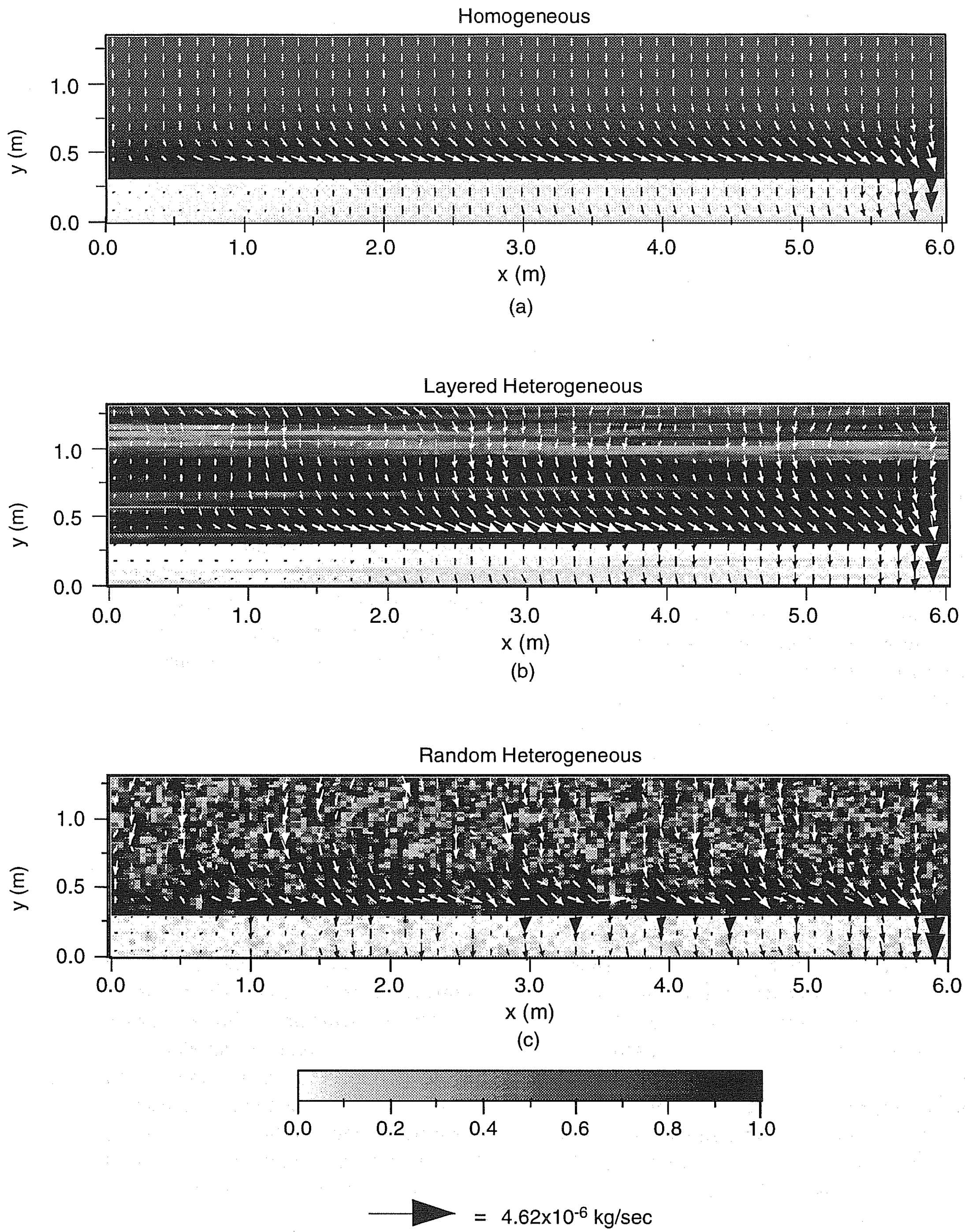

Figure 1. Simulated steady-state liquid saturations and mass flow vectors: a) homogeneous field, b) layered heterogeneous field (realization 7), and c) random heterogeneous field (realization 7). The domains are tilted 5 degrees clockwise.

flow exiting the bottom right corner, which is connected to a saturated boundary, must equal the total mass flow entering the system from infiltration.

The resulting saturation profiles and mass flow vectors for the different fields are very distinct. The homogeneous field (Figure 1(a)) displays a fairly uniform saturation distribution in the fine layer, with saturation increasing near the interface of the fine and coarse layers. Water flow is primarily vertically downward except at the interface, where lateral

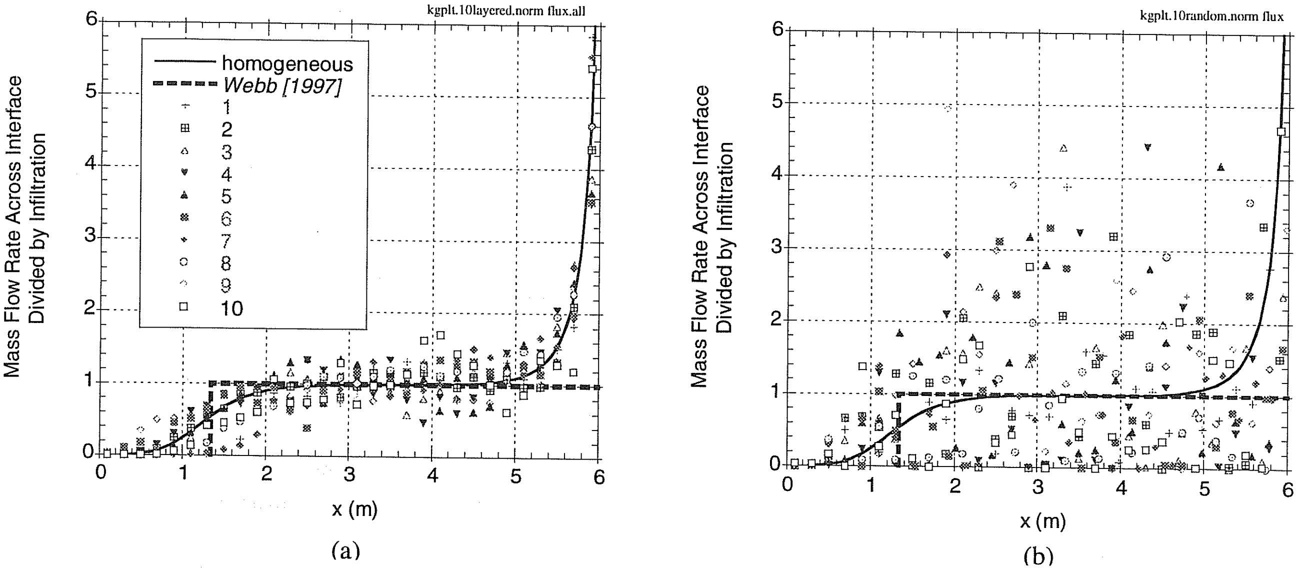

Figure 2. Mass flow rate across the interface of the fine and coarse layers divided by the infiltration rate (1 mm/day): a) ten layered heterogeneous realizations b) ten random heterogeneous realizations. The homogeneous solution and modified solution of *Ross* [1990] (detailed in *Webb* [1997]) are also shown.

diversion exists. In addition to diversion at the interface, the layered heterogeneous field shown in Figure 1 (b) also exhibits regions of lateral diversion *within* the fine layer of soil. Thin lenses of high permeability (and low liquid saturation) within the fine layer at $y \sim 1$ m act as localized capillary barriers that contribute to additional lateral diversion. The random heterogeneous field shown in Figure 1(c) yields localized channeling of downward flow through high permeability zones. Also, the "salt and pepper" saturation distribution is indicative of the highly variable permeability field that causes the localized flow in the random heterogeneous field. The channeled flow results in numerous locations of breakthrough along the interface of the fine and coarse layers.

The diversion capacities of the different fields is quantified in Figure 2, which displays the mass flow rate of water entering the coarse layer divided by the infiltration rate as a function of distance along the interface. Figure 2(a) shows that the results of the layered heterogeneous fields bound those of the homogeneous field. The distance that water is diverted before flowing into the coarse layer is twice that of the homogeneous field in realization 7, but the diversion distance is approximately half that of the homogeneous field in realization 9. The homogeneous results appear to give a reasonable approximation to the mean behavior of the ten layered heterogeneous realizations. In contrast, the random heterogeneous field (Figure 2(b)) displays a chaotic breakthrough pattern and a diversion distance that is shorter than the homogeneous model in nearly all the realizations. The results of a semi-analytical solution using a modified formulation of *Ross* [1990] as described in *Webb* [1997] is also shown, where appropriate van Genuchten functions have been used. Note that the no-flow right boundary causes significantly higher mass flow rates along the right side of the domain, but for regions greater than one meter from the right boundary, the influence of the right boundary is minimal.

Another useful means of quantifying the performance of capillary barriers is to define a cumulative breakthrough ratio, χ, by integrating the mass flow of water entering the coarse layer with respect to distance along the interface and dividing this quantity by the integrated infiltration with respect to distance along the surface:

$$\chi = \frac{\int_0^x \dot{m}(x)\, dx}{\int_0^x q\,(x)\, dx} = \frac{1}{q\,x}\int_0^x \dot{m}(x)\, dx \qquad (3)$$

where *m(x)* is the mass flow rate of water entering the coarse layer at a location x and q is the infiltration rate (assumed constant in this study). Figure 3 shows the mean cumulative breakthrough ratio for all realizations of the random and layered heterogeneous systems. The homogeneous results are also shown for comparison. The homogeneous results are quite similar to the mean cumulative breakthrough ratio curve of all the layered heterogeneous realizations, indicating that the homogeneous model may be used to predict the average behavior of layered heterogeneous systems. The mean cumulative breakthrough curve for the random

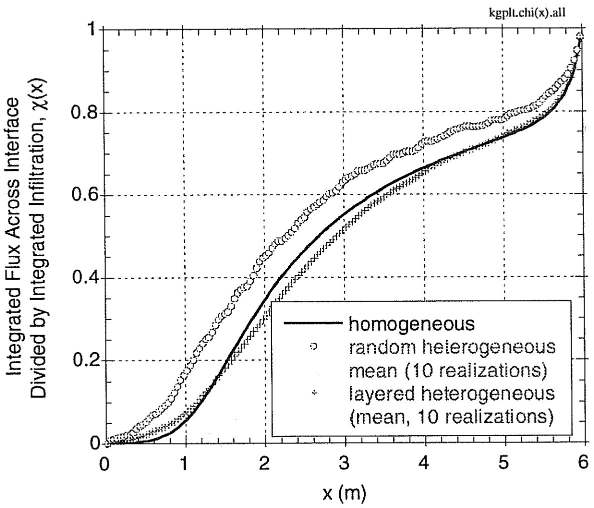

Figure 3. Mean of the cumulative breakthrough ratio curves (Equation (3)) for all simulations.

heterogeneous realizations lies above the homogeneous curve for all locations, indicating that the homogeneous model over-predicts the diversion capacity of random heterogeneous fields. The random heterogeneous systems perform poorly because of the numerous preferential pathways that channel liquid downward, causing an immediate breakthrough in nearly all of the realizations.

Figure 4 shows the liquid saturation profile and mass flow vectors for a homogeneous simulation with a wavy interface. The amplitude of the wave, A, is 0.1 m and the frequency, n, is 5. The breakthrough into the coarse layer is restricted primarily to the troughs of the wavy interface. This feature can be exploited by designing capillary barriers that have troughs, or drainage points, between areas that need to be isolated, such as waste packages.

One final comment should be made regarding the computational performance of each of the simulations. The homogeneous and layered heterogeneous simulations took on the order of several hours to reach steady-state from residually saturated initial conditions. However, the random heterogeneous field had difficulty reaching steady-state from residually saturated initial conditions. A uniform initial saturation greater than residual was imposed to allow the random heterogeneous simulation to reach steady-state. Different initial saturations were imposed, and while the results were identical, the duration and number of time steps required to reach steady-state were highly dependent on the value of the initial saturation.

4. Conclusions

Simulations have been performed to investigate the effects of heterogeneities on the performance of capillary barriers. Homogeneous, layered heterogeneous, and random heterogeneous representations of a system comprised of a fine soil layer overlying a coarse gravel layer were simulated to determine the amount of lateral diversion above the coarse layer under steady-state infiltration conditions.

Multiple realizations of the layered heterogeneous system resulted in breakthrough curves that bounded the homogeneous results. Realizations that consisted of highly stratified regions in the fine layer yielded the least amount of breakthrough in upstream regions due to additional local capillary barrier effects in the fine layer. Realizations that consisted of a fine layer that was graded from coarse at the top to fine at the bottom experienced earlier breakthrough relative to the homogeneous simulation due to increased saturations and decreased capillarity above the interface of the fine and coarse layers. All realizations of the random heterogeneous system resulted in earlier breakthrough compared to the homogeneous and layered heterogeneous runs. Preferential vertical pathways channeled flow that produced numerous localized regions of breakthrough into the coarse layer.

These results indicate that engineered capillary barriers may be improved through emplacement and packing methods that induce highly stratified features within the fine layer of a capillary barrier system. In addition, homogeneous models can be used to estimate the average behavior of layered heterogeneous systems with reasonable accuracy. The modified analytical solution of *Ross* [1990], which predicts diversion capacity for homogeneous systems [*Webb*, 1997], accurately predicted the mean diversion capacity of the layered heterogeneous systems. However, results also indicate that simple homogeneous simulations will over-predict the diversion capacity of capillary barriers if the fine layer consists of randomly distributed properties that act to channel the downward flow through preferential pathways.

Simulations of capillary barriers have also been performed using non-uniform interfaces between the fine and coarse layers. "Wavy" interfaces have been generated using periodic functions of varying amplitude and frequency. The resulting interfaces can range from smooth parabolic to highly irregular and "jagged" interfaces. Preliminary results of these simulations indicate that breakthrough into the coarse layer is contained primarily in the troughs of wavy interfaces.

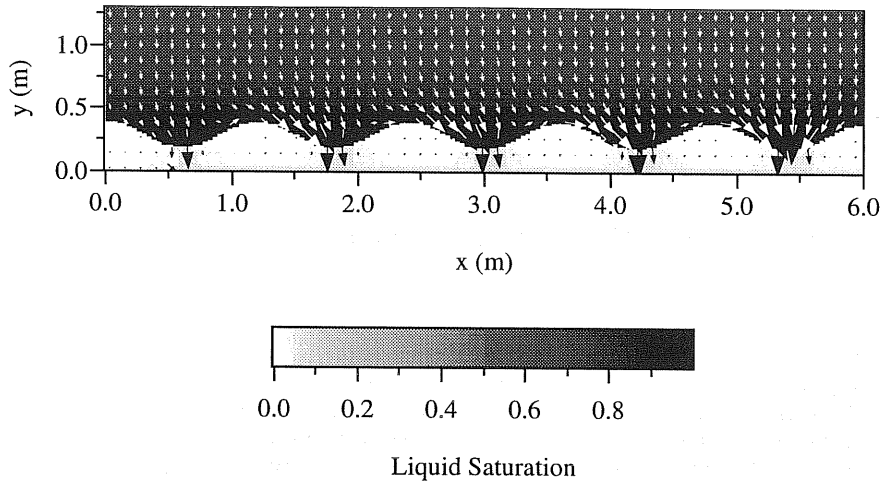

Figure 4. Liquid saturation and mass flow vectors for wavy interface simulation (A=0.1, n=5; Equation (2)).

This design may be useful in waste isolation by providing drainage points between waste packages.

Acknowledgments

The authors would like to thank Sean McKenna, Ray Finley, Eric Ryder, Mike Wilson, and Peter Davies for their discussions and review of this work. Sandia is a multiprogram laboratory operated by Sandia Corporation, a Lockheed Martin Company, for the United States Department of Energy under Contract DE-AC04-94AL85000.

References

Deutsch, C.V. and A.G. Journel, *GSLIB: Geostatistical Software Library and User's Guide*, Oxford University Press, New York, 1992.

Ho, C.K. and K.S. Udell, An Experimental Investigation of Air Venting of Volatile Liquid Hydrocarbon Mixtures from Homogeneous and Heterogeneous Porous Media, *J. Contam. Hydrol.,* 11, 291-316, 1992.

Morris, C.E. and J.C. Stormont, Capillary Barriers and Subtitle-D Covers: Estimating Equivalency, *J. Env. Eng.-ASCE*, 123(1), 3-10, 1997.

Oldenburg, C.M. and K. Pruess, On Numerical Modeling of Capillary Barriers, *Water Resour. Res.*, 29, 1045-1056, 1993.

Prindle, R.W. and P.L. Hopkins, On Conditions and Parameters Important to Model Sensitivity for Unsaturated Flow Through Layered, Fractured, Tuff: Results of Analyses for HYDROCOIN Level 3 Case 2, *SAND89-0652*, Sandia National Laboratories, Albuquerque, NM, 1990.

Pruess, K., TOUGH User's Guide, *LBL-20700*, Lawrence Berkeley Laboratory, Berkeley, CA, 1987.

Pruess, K., TOUGH2—A General-Purpose Numerical Simulator for Multiphase Fluid and Heat Flow, *LBL-29400*, Lawrence Berkeley Laboratory, Berkeley, CA, 1991.

Ross, B., The Diversion Capacity of Capillary Barriers, *Water Resour. Res.*, 26, 2625-2629, 1990.

Selker, J., Design of Interface Shape for Protective Capillary Barriers, *Water Resour. Res.*, 33, pp. 259-260, 1997.

Stormont, J.C., The Performance of Two Capillary Barriers During Constant Infiltration, in Landfill Closures, *ASCE Geotechnical Special Publication No. 53*, Edited by Bunn and Singh, pp. 77-92, 1995.

Warrick, A.W., P.J. Wierenga, and L. Pan, Downward Water Flow Through Sloping Layers in the Vadose Zone: Analytical Solutions for Diversions, *J. Hydrology*, 192, 321-337, 1997.

Webb S.W., Selection of a Numerical Unsaturated Flow Code for Tilted Capillary Barrier Performance Evaluation, *SAND96-2271*, Sandia National Laboratories, Albuquerque, NM, 1996.

Webb, S.W., Generalization of Ross' Titlted Capillary Barrier Diversion Formula for Different Two-Phase Characteristic Curves, *Water Resour. Res.*, 33(8), 1855-1859, 1997.

Webb, S.W., J.T. McCord, and S.F. Dwyer, The Applicability of the HELP Model in Predicting Tilted Capillary Barrier Performance, in Proceedings of the *1997 International Containment Technology Conference and Exhibition*, St. Petersburg, FL, 1997.

Wilson, M.L., Lateral Diversion in the PTn Unit: Capillary-Barrier Analysis, in Proceedings of the *1996 International High Level Radioactive Waste Management Conference*, Las Vegas, NV, 111-113, 1996.